data

MDPI

Article

Dataset of Gravity-Induced Landforms and Sinkholes of the Northeast Coast of Malta (Central Mediterranean Sea)

Stefano Devoto [1,*], Linley J. Hastewell [2], Mariacristina Prampolini [3] and Stefano Furlani [1]

[1] Department of Mathematics and Geosciences, University of Trieste, 34127 Trieste, Italy; sfurlani@units.it
[2] School of the Environment, Geography and Geosciences, University of Portsmouth, Portsmouth PO1 3HE, UK; linley.hastewell@port.ac.uk
[3] National Research Council, Institute of Marine Sciences, 40129 Bologna, Italy; mariacristina.prampolini@bo.ismar.cnr.it
* Correspondence: stefano.devoto2015@gmail.com

Abstract: This study investigates gravity-induced landforms that populate the North-Eastern coast of Malta. Attention is focused on tens of persistent joints and thousands of boulders associated with deep-seated gravitational slope deformations (DGSDs), such as lateral spreads and block slides. Lateral spreads produce deep and long joints, which partially isolate limestone boulders along the edge of wide plateaus. These lateral spreads evolve into large block slides that detach thousands of limestone boulders from the cliffs and transport them towards the sea. These boulders are grouped in large slope-failure deposits surrounding limestone plateaus and cover downslope terrains. Gravity-induced joints (n = 124) and downslope boulders (n = 39,861) were identified and categorized using Google Earth (GE) images and later validated by field surveys. The datasets were digitized in QGIS and stored using ESRI shapefiles, which are common digital formats for storing vector GIS data. These types of landslides are characterized by slow-moving mechanisms, which evolve into destructive failures and present an elevated level of risk to coastal populations and infrastructure. Hundreds of blocks identified along the shore also provide evidence of sinkholes; for this reason, the paper also provides a catalogue of sinkholes. The outputs from this research can provide coastal managers with important information regarding the occurrence of coastal geohazards and represent a key resource for future landslide hazard assessment.

Dataset: https://doi.org/10.6084/m9.figshare.14980215.v1

Keywords: gravity-induced joint; megaclast; lateral spread; block slide; GE image; Malta

Citation: Devoto, S.; Hastewell, L.J.; Prampolini, M.; Furlani, S. Dataset of Gravity-Induced Landforms and Sinkholes of the Northeast Coast of Malta (Central Mediterranean Sea). *Data* **2021**, *6*, 81. https://doi.org/10.3390/data6080081

Academic Editor: Jamal Jokar Arsanjani

Received: 12 July 2021
Accepted: 28 July 2021
Published: 31 July 2021

1. Introduction

Large landslides occur in several coastal areas of Europe and are particularly common in Spain [1], Greece [2], Italy [3–6], and Slovenia [7]. These phenomena frequently affect coastal facilities and are often triggered by human intervention or by the increasing occurrence of extreme meteorological events.

Malta is one of the Mediterranean nations most affected by landsliding [8]. Within the Maltese archipelago, coastal landslides are widespread and active in north Malta [9–12], in east Gozo [13], and Filfla [14]. Most are large landslides and affect extensive sectors of the coast, including the limestone plateaus, plunging cliffs, structural caprocks, and underlying clay terrains. Extensive mapping activities carried out in North-West Malta and Gozo have classified these large landslides as lateral spreads and blocks slides [9,13]. These landslide types are widespread in North Malta and relate directly to the distinct geological setting which features several SW–NE oriented faults [10,12]. These faults degrade the limestone rock masses located along the edges of the Marfa Ridge peninsula and the

Mellieha plateau [12]. Lateral spreads [15] and block slides [16] are characterized by slow, progressive movement and develop into distinct geostructural coastal features, such as persistent joints, bulges, and large boulder accumulations. The low rate of deformation of Maltese rock spreads and block slides, and the associated gravity-induced landforms they produce, are diagnostic for categorizing them as DGSDs [17,18]. The investigations and mappings of these surface features are crucial for the description and interpretation of DGSDs, as reported by [19]. Gravity-induced joints are distinctive landforms that accompany rock spreading and occur along the external sector of four wide plateaus that populate the coastline of north Malta [12,20]. These discontinuities run parallel to plateau cliffs, as illustrated in the northern sector of Anchor Bay [20–22]. Alternatively, they form a complex network of discontinuities, as displayed in the external sectors of the Marfa Ridge peninsula and at the Il-Qarraba caprock [20,22].

These joints are deep and can exceed 150 m in length, partially isolating large rock masses [22]. These are prone to detachment from the cliffs causing catastrophic failure, thus representing a considerable geohazard. The extensive cracking process is caused by the opposing geotechnical properties of the rigid Upper Coralline Limestone (UCL) Formation and underlying Blue Clays (BC) [23]. These two rock units are abundant in northern Malta in contrast to southern Malta (Figure 1), where older rock units such as the Globigerina Limestone (GL) Formation and the Lower Coralline Limestone (LCL) Formation dominate [23,24]. This superimposition of UCL and underlying BC in North Malta is the key predisposing factor for lateral spreading [10,12].

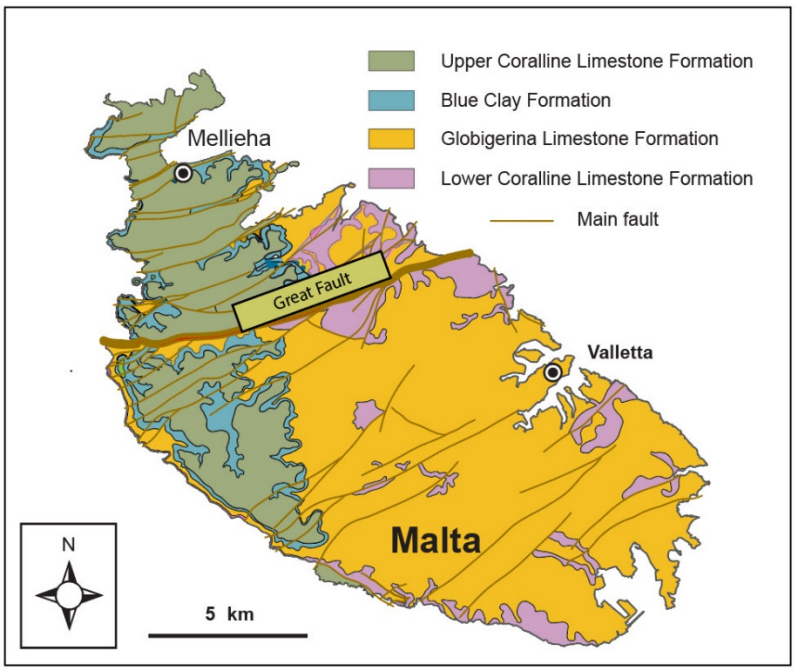

Figure 1. Geological map of Malta.

These lateral spreads frequently evolve into destructive failures that detach huge boulders from the plateau cliffs. Thousands of UCL boulders are scattered downslope forming unique landscapes called Rdhum by the Maltese (Figure 2) [9,10,12,22]. Block slides slowly transport boulders downslope towards the sea [20,21]. It is proposed that most of the detached boulders have been transported along BC slopes over the course of the last 20,000 years, as dated in two coastal sites by [25], when the Maltese sea level was approximately 130 m lower than at present [26].

Figure 2. View of an extensive coastal boulder deposit (Rdhum landscape) in north Malta.

Previous contributions towards developing a deeper understanding of landslides in Malta have focused predominantly on its North-West sector, which caters for the valuable tourist industry, with sandy beaches as well as a natural protected area, which is rich in geoheritage and displays wide geomorphological variety and outstanding geological landscapes [27,28]. A detailed landslide inventory map (LIM) included in a 1:7500 scale geomorphological map was produced in 2012, covering the North-West coast stretching between the Marfa Ridge peninsula and Il-Pelegrin Promontory [9]. Additionally, Piacentini et al. [29] devised a landslide susceptibility map using the weight of evidence (WOS) method, but this study was limited only to a 4 km coastal stretch of North-West Malta. Findings based on outputs from differential GNSS surveys [21] and satellite synthetic aperture radar (SAR) interferometry [30] have addressed the temporal evolution of the North-West DGSDs. Conversely, few papers are devoted to DGSDs on the neglected North-East coast, as it is wrongly assumed that North-Eastern landslides are less extensive and less hazardous. Prampolini et al. [31] produced an integrated geomorphological map of the northern part of Malta, although it only provides a general overview of North-East landslides due to its scale (1:25,000). Another study used geophysical methods for the investigation of a DGSD affecting the coastal village of Xemxija, where a large lateral spread and associated persistent joints resulted in considerable structural damage to a local church [32].

This study is comprised of an inventory and characterization of gravity-induced landforms performed by means of GE image analysis and subsequent validation from field surveys. Geomorphological mapping based on aerial-photo interpretation is a widely used method for mapping coastal areas and cliffs, particularly where steep escarpments and landslides make sites dangerous or unsafe for extensive field mapping activities [22,33,34].

The outputs of this work provide a complete inventory of landslide-derived landforms situated on the eastern coastal areas located between the Marfa Ridge peninsula and Selmun promontory. The spatial distribution of gravity-induced joints is crucial for the recognition of areas affected by lateral spreading and can provide vital information about their internal perimeter and rock masses that can evolve into catastrophic failures.

Such progressive, unstable rock masses pose a risk to public safety and have the potential to damage coastal areas of high economic, cultural and social value as well as

associated infrastructure [35]. An improved understanding of the spatial extent of these geohazards enables mitigating coastal management practices to be implemented to reduce risk exposure in areas identified as vulnerable.

Finally, we identified, mapped, and categorized thousands of coastal boulders performing an aerial image interpretation using GE images. Furthermore, creating a boulder inventory of coastal deposits can provide useful information on block slide evolution and possible insights regarding the position and depth of its slip surface.

These data were digitized in QGIS software (https://qgis.org/en/site/, accessed on 30 May 2021) and stored as ESRI shapefiles. These data represent an important source of information for slope stability analysis and for the production of a new, large-scale geomorphological map.

2. Study Area

The study area is located in the North-East part of Malta (Figure 3A), which is the largest island of the Maltese archipelago. The study area is located in the Mellieha municipality, which is the northernmost town on the Malta island (Figure 3B). This study covers a total surface area of 2.8 km^2, stretching from the northern coast of L-Ahrax to the southern coast of Selmun headland. The study area also includes St Paul's Islands.

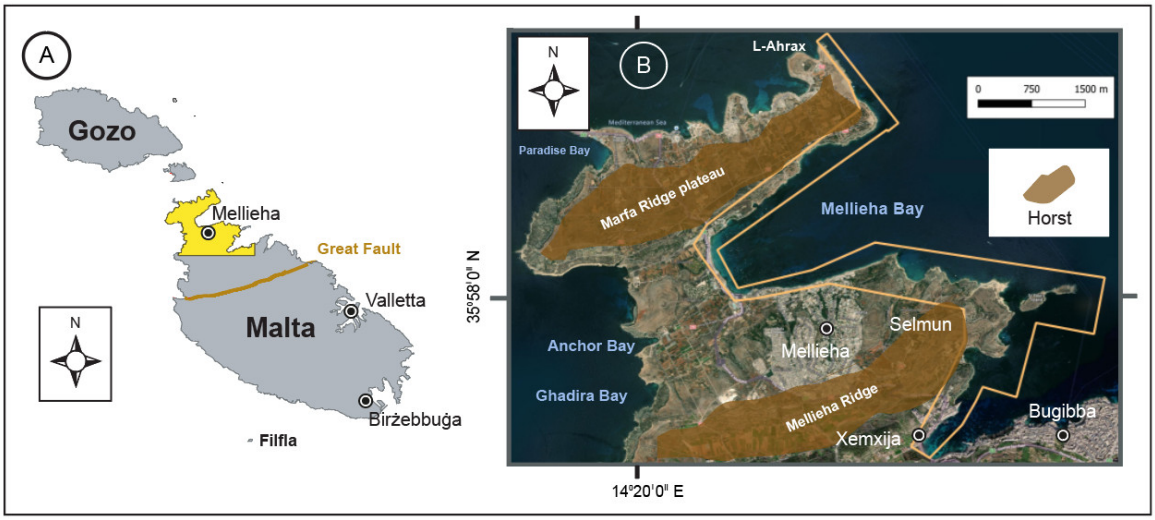

Figure 3. (**A**) Map of the Maltese islands; and (**B**) location of the study area. The orange polygon in B indicates the study area.

The study area includes two ridges and two lowland areas, demonstrating a horst-and-graben topography [36]. From North to South, it includes the eastern sector of the Marfa Ridge peninsula and the headland of Selmun, where the urban areas of Mellieha and Xemxija lie (Figure 4). The Marfa Ridge peninsula is characterized by a wide UCL plateau, which is weakened by a SW–NE oriented fault (Figure 4) located in the northern part of Mellieha Bay and tens of persistent joints formed by lateral spreading (Figure 5A), as reported by [31]. These discontinuities are located along the external sector of the UCL plateau and favor landsliding, as witnessed by the large boulder deposits called Rdhum il-Hmar and Rdhum tal-Madonna (Figure 4). The headland of Selmun is part of the Mellieha Ridge and separates the structural depressions of Mellieha Bay and St Paul's Bay [36], which follow the SW–NE oriented faults that characterize North Malta (Figure 4). UCL rock masses dominate with respect to other sedimentary rock formations (Figure 6). The abundance of UCL in the study area and the presence of underlain BC slopes along the shoreline (GL rock masses represent less than 10% of the total study area) represent the main predisposing factors for the occurrence of lateral spreading, rock falls, and block slides along the northeastern coast of Malta. GL layers occur along the shoreline

in the northern sector of the Selmun promontory, between Mgiebah Bay and Blata I-Badja. GL shore platforms occur as sub-horizontal terraces [37], and are frequently backed by large slope-failure deposits detached by upland UCL relief, which reaches an elevation of 110 m near Selmun Palace [38]. A structural and lithological control is evident in the south and south-eastern sectors of the Selmun headland, where a network of faults crosses Ras il-Mignuna, Mistra Bay and low-lying GL slopes in Mistra [31,38]. The above-cited faults cause the alternation of a steep UCL escarpment, GL rock masses, and gentle BC terrains, which favor landsliding and subsidence phenomena (Figure 5B).

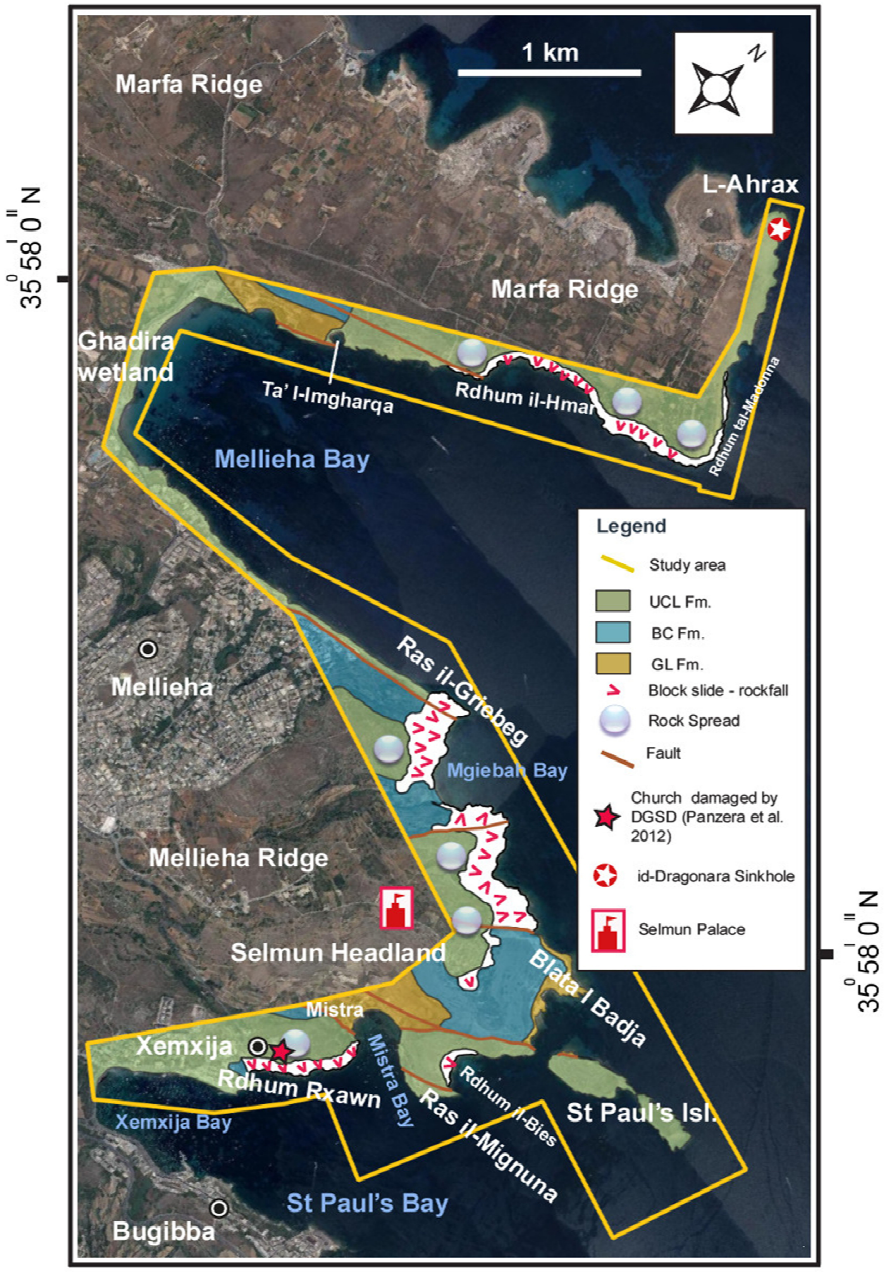

Figure 4. Geological and landslide map of the study area on the northeastern coast of Malta.

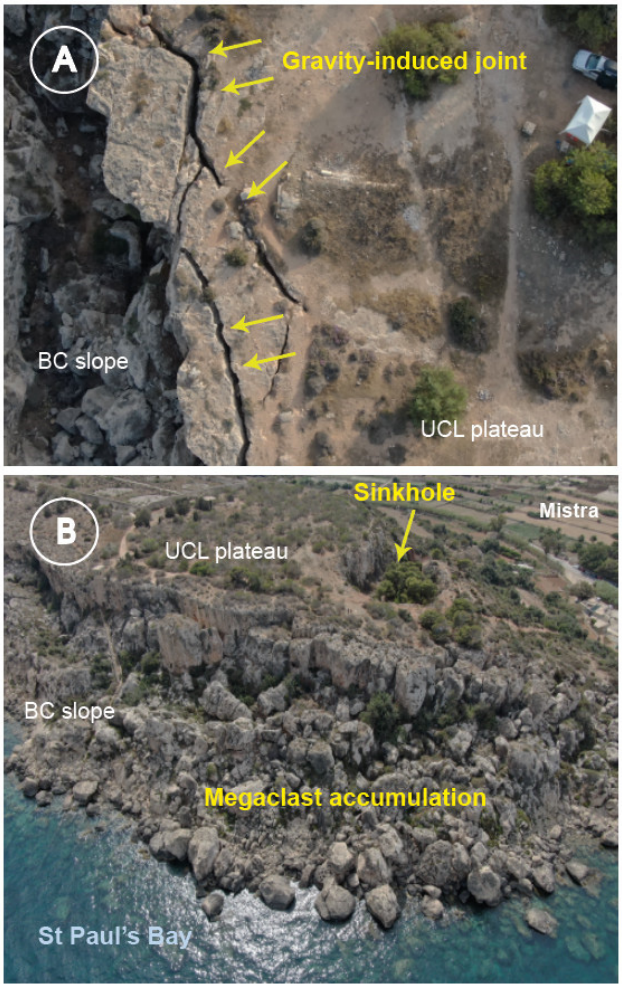

Figure 5. (**A**) Drone-derived image of gravity-induced joints along the Marfa Ridge plateau; and (**B**) drone-derived photo of Rdhum Rxawn, where a large slope-failure deposit occurs downslope between St Paul's Bay and the UCL plateau.

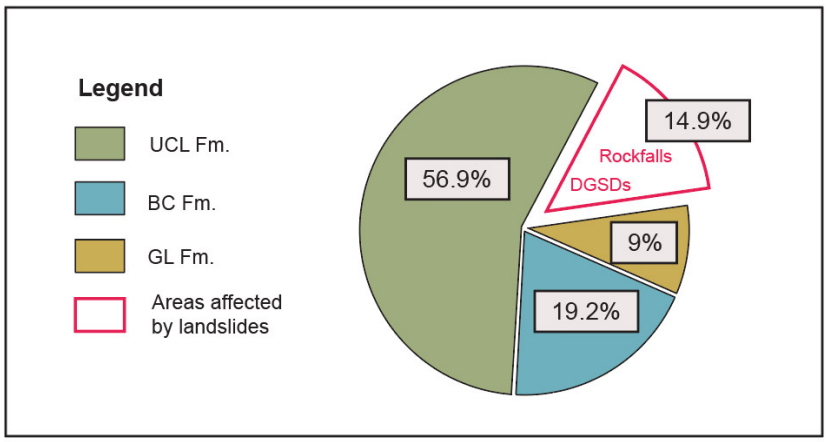

Figure 6. The distribution of landslides and Maltese geological formations along the northeastern coast of Malta with respect to the total surface of the study area.

Rockfalls are common from plunging cliffs at Ras-il Mignuna as well as DGSDs at Rdhum il-Bies and Rdhum Rxawn [38]. Figure 5B shows a panoramic view of a large boulder accumulation generated by block slides and lateral spreads affecting the rocky

slopes at Rdhum Rxawn. The literature search [31,32,38,39] shows that the area affected by DGSDs and other types of landslides covers 14.9% of the study area, as shown in Figure 6.

Two karst depressions were recently described and mapped in the study area [31,37,38]. A sea-flooded sinkhole called Coral lagoon or id-Dragonara is located on the northern part of the Marfa Ridge plateau (Figure 4), and was recently described by [39]. Another large sinkhole occurs near Mistra (Figure 5B), and was mapped by [31,38]. According to genetic classification developed by [40], these subsidence landforms can be classified as bedrock collapse sinkholes.

3. Materials and Methods

This study investigates a series of gravity-induced landforms on the north-eastern coast of Malta using GE images. The data were digitized and stored in QGIS 3.10 A Coruña (QGIS Development Team, QGIS Geographic Information System, Open-Source Geospatial Foundation Project, https://www.qgis.org/en/site/forusers/visualchangelog310/index.html, accessed on 30 May 2021).

3.1. Design of the Dataset

Four datasets were produced using four ESRI shapefiles. For this reason, each dataset corresponds to a respective ESRI shapefile. The ESRI Shapefile is a digital format for storing vector GIS data. Two datasets related to gravity-induced landforms were produced ("Joint_NE" and "Superblock_NE"), along with one dataset of boulders mainly related to landslides ("Size_megaclasts_NE") and a further dataset of sinkholes ("Sinkhole_NE"). Table 1 includes shapefile names and the associated datasets, lists the data structure information and a brief explanation of each dataset.

Table 1. Shapefile names and descriptions.

Shapefile Name	Dataset	Data Structure	Explanation
Joint_NE	Gravity-induced joints	Line	Location and persistence characterization of induced-gravity joints
Size_megaclasts_NE	Blocks and megablocks	Point	Location and size categorization of boulders with axis not exceeding 100 m.
Superblock_NE	Superblocks	Polygon	Location and size categorization of boulders with major axis exceeding 100 m
Sinkhole_NE	Sinkholes	Polygon	Location and type categorization according to [40]

Each shapefile contains different attributes. The shapefile named "Joint_NE" contains the following attributes: (i) Length; (ii) Pers class (Table 2). Tables 3 and 4 list the attributes and additional details of the aforementioned shapefiles related to boulders.

Table 2. Attributes of the shapefile named "Joint_NE".

Attribute Name	Data Type	Explanation	Unit	Comment
Length	Number	Length of joint	m	Number of decimal places = 0
Pers class	Text	Length category	ISRM [1] category	Number of classes = 5

[1] ISRM—International Society for Rock Mechanics.

Table 3. Attributes of the shapefile named "Size_megaclasts_NE".

Attribute Name	Data Type	Explanation	Comment
Type	Text	Size category	Number of classes = 2
Origin	Text	Landslide/sinkhole type	Number of classes = 5

Table 4. Attributes of the shapefile named "Superblock_NE".

Attribute Name	Data Type	Explanation	Comment
Type	Text	Size category	Number of classes = 1
Length	Number	Length of main axis	Number of decimal places = 0
Origin	Text	Landslide type	Number of classes = 1

The shapefile named "Sinkhole_NE" contains the following attributes: (i) Type; (ii) S_Shape; (iii) Position. Table 5 provides the description of attributes.

Table 5. Attributes of the shapefile named "Sinkhole_NE".

Attribute Name	Data Type	Explanation	Comment
Type	Text	Sinkhole category	Number of classes = 2
S_Shape	Text	Shape of sinkhole	Number of classes = 2
Position	Text	Sinkhole location	Number of classes = 2

3.2. Methods for Data Compilation

To compile the datasets related to joints and boulders, a literature search was completed, along with a visual interpretation of GE images, and field surveys carried out in June 2021. Preliminary investigations were dedicated to reviewing and analyzing the relevant literature, including scientific papers published on the study area and existing geological and geomorphological maps. Subsequently, gravity-induced landforms were identified and mapped using visual interpretation of GE images. Most attributes were determined exclusively using GE images, whereas field surveys were performed for validating GE observations and for the detection of joints not observed in GE images. The field surveys were not conducted simultaneously with GE detection of landforms due to travel restrictions linked to the Coronavirus pandemic.

3.2.1. Gravity-Induced Joint Data

We recognized gravity-induced joints and established their major property, such as persistence values. Persistence is the term used to define joint length [41]; its value was expressed in meters. The persistence values were listed in the attribute "Length" (Table 2). Table 6 lists the five text names used in the attribute "Persistence class" (Table 2), which corresponds to ISRM persistence categories [41]. Each ISRM category defines a joint length (third column of Table 6).

Table 6. "Persistence class" text names and corresponding ISRM categories [41].

Text Names	ISRM Category	Joint Length [m]
very low	Very low persistence	<1
low	Low persistence	1–3
medium	Medium persistence	3–10
high	High persistence	10–20
very high	Very high persistence	>20

GE image analysis and field surveys were not used to quantify joint apertures, due to the reduced level of image accuracy in defining cm values and safety reasons.

3.2.2. Megaclast Data

Finally, we used GE images for the detection of boulders and their size categorizations using the methodology proposed by Bruno and Ruban [42]. This method was already used for the investigation of coastal megaclast deposits [22,43]. For this size classification, megaclasts are detrital sedimentary particles larger than 1 m in size. Depending on the main axis dimension, this methodology subdivides megaclasts into: (i) blocks (1–10 m);

(ii) megablocks (10–100 m); (iii) superblocks, when one axis length exceeds 100 m. These megaclasts were digitized using two shapefiles (Table 7).

Table 7. Text names used for attribute named "Type".

Text Names	"Size_megaclast_NE" Shapefile	"Superblock_NE" Shapefile
Block	X	-
Megablock	X	-
Superblock	-	X

Superblocks were digitized as polygons and stored in the shapefile called "Superblock_NE". Conversely, we digitized blocks and megablocks as points. These data were stored in the shapefile called "Size_megaclasts_NE". The attribute "Type" classifies each megaclast using the above-cited method [42]. Table 7 lists the three text names used for the attribute "Type".

The two aforementioned shapefiles also include an attribute named "Origin", which contains information regarding the different types of landslides or sinkholes that detached, moved or produced the single megaclast. Table 8 lists the text names used for the attribute "Origin". Landslide types are classified according to [44].

Table 8. Text names used for the attribute "Origin".

Text Name	Landslide Type	Sinkhole Type
Block slid	Block slide	-
Rockfall	Rock fall	-
Topple	Rock topple	-
B C Sink	-	Bedrock collapse sinkhole
Undetermined	-	Sinkhole not categorized

3.2.3. Sinkhole Data

The shapefile "Sinkhole_NE" contains three attributes. Table 9 lists the text names used for the attributes "Type", "S_Shape", and "Position". Sinkholes were recognized and classified combining GE analysis and a literature search [31,38,39]. These analyses were later validated by field visits carried out in June 2021.

Table 9. Text names used for attributes of "Sinkholes_NE".

Text Name	Attribute Name	Key/Comment
B C Sink	Type	Bedrock collapse sinkhole
Ind_Sink	Type	The sinkhole was not categorized
Circular	S_Shape	Sinkhole has a form of a circle
Oval	S_Shape	Sinkhole has an elongated outline
Inland	Position	Sinkhole is located inland
Sea	Position	The sinkhole floor is located offshore

4. Results and Inventory Statistics

4.1. Gravity-Induced Joint Data

The GE analysis carried out on gravity-induced joints enabled the identification and categorization of a total population of 124 discontinuities (Table 10), located mostly (n = 82) along the edge of the Marfa Ridge plateau.

Table 10. Gravity-induced joint population and their persistence categories according to ISRM.

	Total	Very Low (<1 m)	Low (1–3 m)	Medium (3–10 m)	High (10–20 m)	Very High (>20 m)
Gravity-induced joint	124	4	18	46	30	26

Over 50 joints exceeded ten meters in length (ISRM categories "High" and "Very High"), demonstrating that lateral spreading is a common landslide type within the study area.

The stretch of the Marfa Ridge coast located between the Tal-Madonna plateau and Rdhum il-Hmar are populated by 66% of the total population of gravity-induced joints. Over 95% of joints located along the Marfa Ridge plateau are orientated parallel to the UCL escarpment, and 81% of them are characterized by "Medium persistence", "High persistence" and "Very high persistence" classes (Figure 7). This orientation confirms the occurrence of lateral spreads and their impact on the edge of UCL rock masses, mainly at Tal-Madonna, and at Rdhum il-Hmar. Four joints exceed 50 m and partially isolate large rock masses which are susceptible to further detachment.

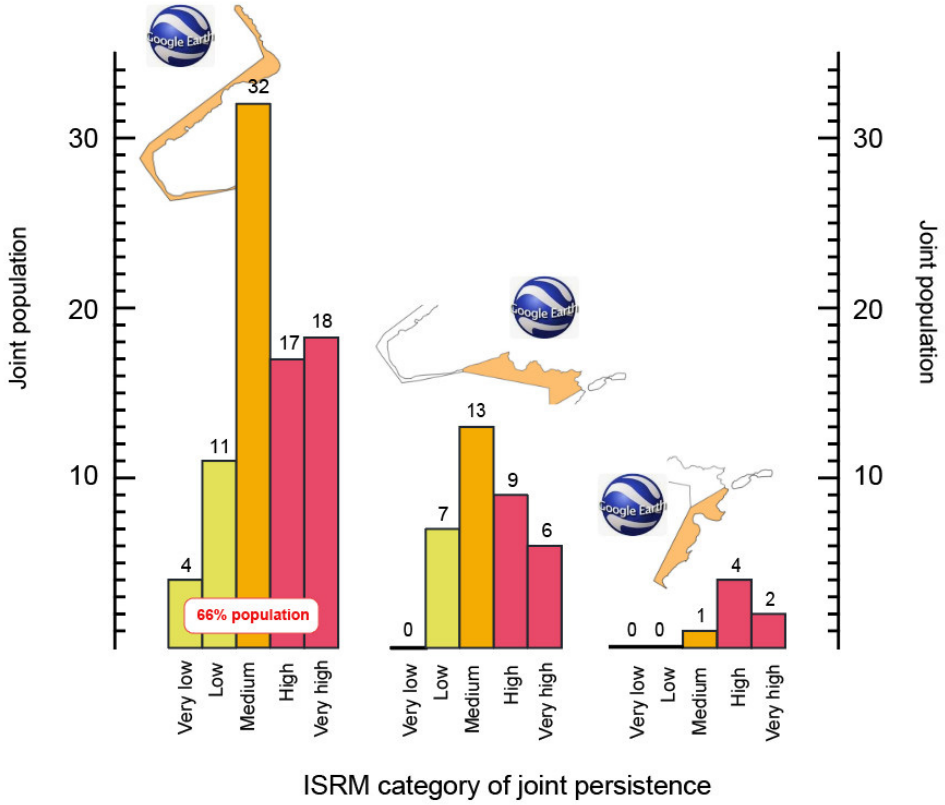

Figure 7. Variation of joint population according to ISRM persistence standards along different sectors of the study area. No gravity-induced joints were detected on St Paul's Islands.

Only seven joints were recognized along the UCL rock masses at Rdhum Rxawn and at Ras-il-Mignuna, but most of them were characterized by "High persistence" or "Very high persistence" values, confirming the landslide risk for the urban area of Xemxija, reported by [32]. Conversely, no joints were detected on the St Paul's Islands, where lateral spreads do not affect plunging cliffs.

4.2. Megaclast Data

A total of 39,861 megaclasts were detected in the study area (Table 11 and Figure 8), with blocks (n = 39,573) dominating with respect to other size categories. Table 11 lists the total population for each size category according to the method developed by [42]. Figure 9 shows that most megaclasts are transported by block slides (Attribute "Origin" in shapefiles "Size_megaclast" (n = 39,860) and shapefile "Superblock_NE" (n = 1)).

Most of the megaclast population (n = 22,768) are located along the northern sector of Selmun headland (Figure 8), where large block slides affect the BC slopes of Ras il-Griebeg

and Blata I-Badja. Analysis indicated a density of 21,003 megaclasts per square kilometer, approximately double that of the other areas affected by DGSDs (see Figure 8).

We counted in the area surrounding Mgiebah Bay 22,644 blocks and 124 megablocks scattered between the shoreline and the UCL plateau, mainly moved by block slides and rockfalls. Rockfalls are abundant at Ras-Il Griebeg, where a fault favors the detachment and collapse of megaclasts from steep cliffs.

Table 11. Megaclast population and size categorization according to [42].

	Total	Block	Megablock	Superblock
Megaclast	39,861	39,573	287	1

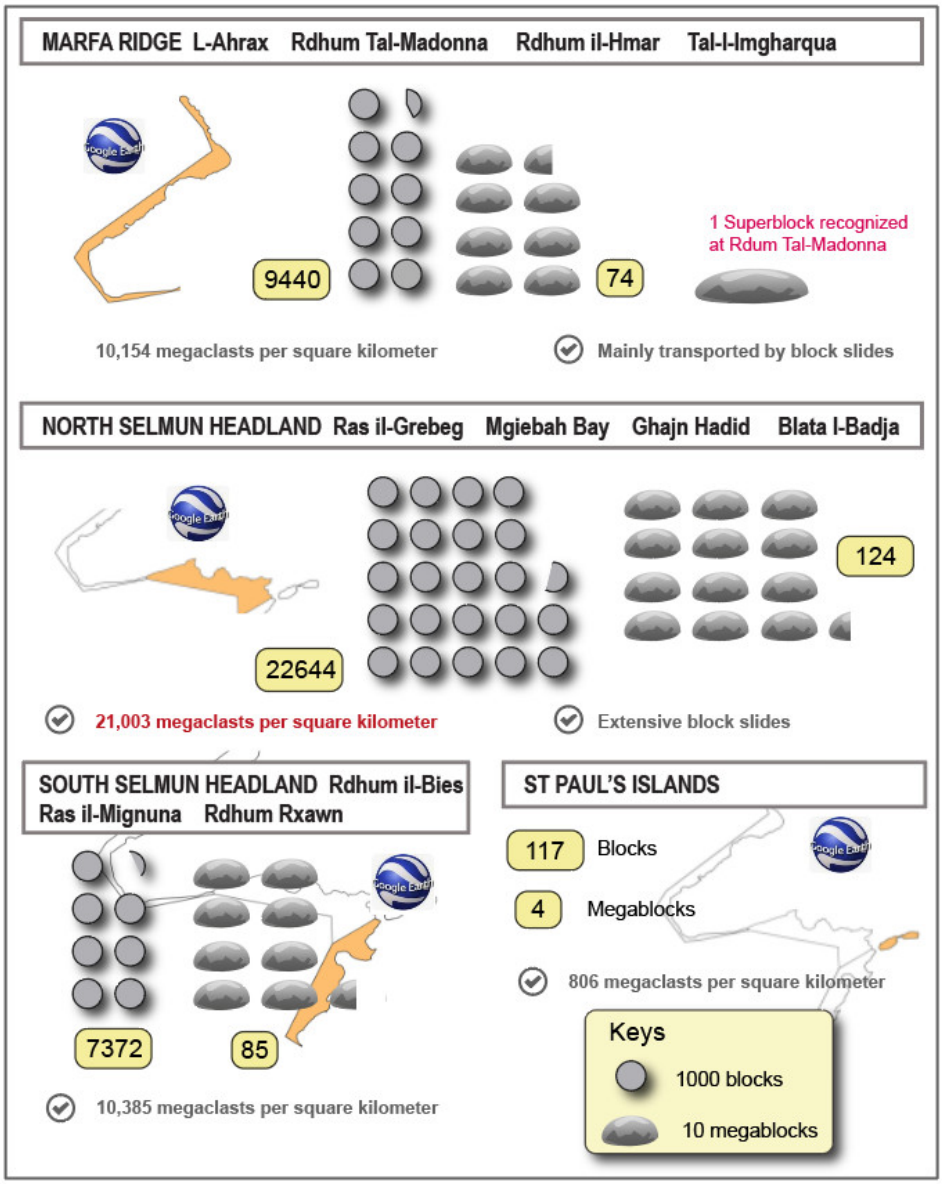

Figure 8. Megaclast size analysis within the study area using GE interpretation.

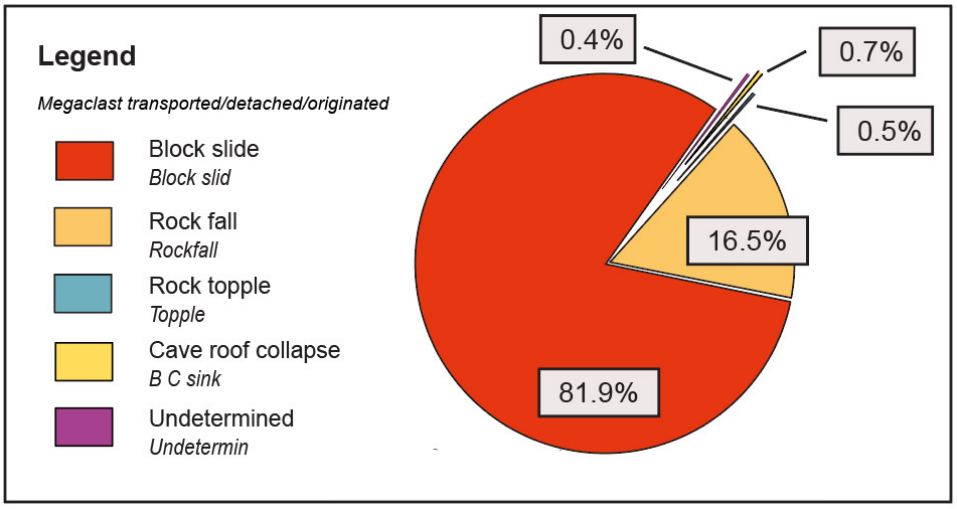

Figure 9. Statistics of attribute "Origin". Over 98% of megaclasts are moved by block slides and rock falls. The latter are frequently collateral landslides of large DGSDs.

Megaclasts are also common in the northern part of the study area. Block slides and rockfalls are common between Rdhum il-Hmar and Rdhum tal-Madonna, where we identified 74 megablocks and 1 superblock. The latter is located downslope near the main scarp and exceeds 346 m in length.

Slope failure accumulations cover large coastal areas of Rdhum il-Bies and Ras il-Mignuna, where 7372 blocks and 85 megablocks were identified. Rockfalls affect plunging cliffs around St Paul's Islands, where 121 megaclasts were detected. Most of them are located along the north-facing side of the main island where a fault that crosses the island [39] facilitates detachment from the plunging cliff.

4.3. Sinkhole Data

A total of five sinkholes were identified using GE images and later validated by field visits carried out in June 2021. Table 12 lists and summarizes the main characteristics.

Table 12. Sinkholes recognized using GE images.

Sinkhole [#]	Location	Type	Shape	Area [m^2]
id-Dragonara Sinkhole	L-Ahrax	Bedrock Collapse Sinkhole	Oval	331
2	L-Ahrax	Bedrock Collapse Sinkhole	Oval	2850
Ta' I-Imgharqa Sinkhole	Mellieha Bay	Bedrock Collapse Sinkhole	Circular	5057
4	Mellieha Bay	Undetermined	Oval	11,501
5	Rdhum Rxawn	Bedrock Collapse Sinkhole	Oval	1733

Sinkholes, such as id-Dragonara, are visited for recreation, swimming, and for their natural beauty by locals and tourists alike [39]. Significantly, the abundance of sinkholes generated by collapse of roof caves demonstrates that sinkholes represent a considerable geohazard, mainly along the shoreline of the Marfa Ridge peninsula. In addition, the Marfa Ridge coast displays a number of elliptical indentations, which suggests that historically there were other sinkholes present that have since been partially eroded by marine processes.

Ta' I-Imgharqa Sinkhole and Sinkhole#4 are aligned along a major fault, which is a precursor to their occurrence. Similarly, at Rdhum Rxawn (Figure 5B) the presence of a sinkhole is the result of collapse mechanisms facilitated by faulting and the impact of lateral spreading affecting the UCL plateau.

5. Conclusions

This study has increased the knowledge and understanding of coastal DGSDs that affect the north-eastern coast of Malta. The research objective was achieved by conducting an inventory and the subsequent analysis of gravity-induced joints and downslope megaclast deposits. We identified, classified and stored in ESRI files 124 gravity-induced joints and 39,861 megaclasts (size greater than 1 m), which originated from lateral spreads, and mainly from block slides, respectively. About 66% of the identified joints occurred along the external sector of the Marfa Ridge plateau, suggesting lateral spreading as the main geohazard for the Marfa Ridge peninsula. These gravity-induced joints, together with faults, occur in coastal areas with steep cliff faces which present a predisposition to develop release surfaces, along which UCL masses which can slide and/or topple. Over 99% of megaclasts identified in the study area were "blocks" (n = 39,573) with 287 megablocks exceeding 10 m in length along one axis, and a huge "superblock" with an axis length exceeding 346 m located at Tal-Madonna. Approximately 82% of megaclasts are transported by block slides, which are abundant in areas underlain with BC terrains such as Ras il-Grieb, Mgiebah Bay, Rdhum Rxawn, Rdhum tal-Madonna and Blata I-Badja. The highest density of megaclasts within the study area was 21,003 megaclasts per square kilometer, which was recorded in the coastal sector between Ras il-Grieb and Blata I-Badja. At this location BC terrains are subjected to marine erosion processes which results in bulging at the cliff toe that frequently produces megaclasts and causes secondary topples or slide failures along the BC slopes.

A second type of geohazard affecting north-eastern Malta is represented by sinkholes. Five sinkholes were identified in accordance with the classification method developed by [40]. These sinkholes are the result of catastrophic cave roof collapse, which we identify as being aligned along geological faults, as demonstrated by Ta' I-Imgharqa in Mellieha Bay. The shapefile outputs created for this study provide the exact location of gravity-induced landforms and sinkholes and represent a significant resource for the production of a new and improved scaled geomorphological map of the north-eastern coast of Malta. At a scale above 1:5000, geomorphological maps are particularly appropriate for regional planning and can also include valuable data for land management activity in urban areas affected by landsliding [45], such as field geotechnical tests, boreholes and spring locations. These detailed cartographic documents are known as engineering geomorphological maps. They are important for the analysis and modeling of local slope stability and they are reliant on accurate data pertaining to slope-damage features. Further development of this research will include the collection of high resolution (HR) images using drones. Drone-derived HR images will be used to produce accurate orthomosaics and 3D models using unmanned aerial vehicle digital photogrammetry (UAV-DP). Such 3D models are fundamental for the examination of aperture values of identified joints, whereas HR images can assist with the detection of megaclasts not visible in GE images. GE images of north-eastern Malta are frequently characterized by wide shadow areas and strong contrasts along the steep cliffs that hinder the identification of blocks located at the foot of vertical escarpments. By incorporating data from a range of sources, it is anticipated that an improved understanding of coastal geohazards within the area will be established.

The focus of this study reflects gravity-induced coastal landforms and sinkholes on the island of Malta. However, the widespread geographical distribution of rock coasts, estimated to be 52% of global shorelines [46], and the increase in coastal populations globally suggest a greater need to assess the risk exposure to coastal geohazards. The methodologies described herein present a useful tool for those responsible for managing public safety in coastal zones of high amenity value that are prone to similar geohazards resulting from geological instabilities.

Author Contributions: Conceptualization, S.D.; investigation, S.D., M.P. and S.F.; methodology, S.D. and L.J.H.; software, S.D.; supervision, S.D. All authors have read and agreed to the published version of the manuscript.

Funding: This research received no external funding.

Data Availability Statement: https://doi.org/10.6084/m9.figshare.14980215.v1 (accessed on 30 July 2021).

Conflicts of Interest: The authors declare no conflict of interest.

Abbreviations

The following abbreviations are used in this paper:

DGSD	Deep-seated Gravitational Slope Deformation
GE	Google Earth
UCL	Upper Coralline Limestone Formation
BC	Blue Clays
GL	Globigerina Limestone Formation
LCL	Lower Coralline Limestone Formation
LIM	Landslide Inventory Map
WOS	Weight Of Evidence
GNSS	Global Navigation Satellite System
SAR	Synthetic Aperture Radar
ISRM	International Society for Rock Mechanics
HR	High Resolution
UAV-DP	Unmanned Aerial Vehicle Digital Photogrammetry

References

1. Mateos, R.M.; Ezquerro, P.; Azañón, J.M.; Gelabert, B.; Herrera, G.; Fernández-Merodo, J.A.; Spizzichino, D.; Sarro, R.; Garcia-Moreno, I.; Bejar-Pizarro, M. Coastal lateral spreading in the world heritage site of the Tramuntana Range (Majorca, Spain). The use of PSInSAR monitoring to identify vulnerability. *Landslides* **2018**, *15*, 797–809. [CrossRef]
2. Ilia, I.; Koumantakis, I.; Rozos, D.; Koukis, G.; Tsangaratos, P. A geographical information system (GIS) based probabilistic certainly factor approach in assessing landslide susceptibility: The case study of Kimi, Euboea, Greece. In *Engineering Geology for Society and Territory*; Lollino, G., Giordan, D., Crosta, G.B., Corominas, J., Azzam, R., Wasowski, J., Sciarra, N., Eds.; Springer: Cham, Switzerland, 2015; Volume 2, pp. 1199–1406.
3. Carobene, L.; Cevasco, A. A large scale lateral spreading, its genesis and Quaternary evolution in the coastal sector between Cogoleto and Varazze (Liguria-Italy). *Geomorphology* **2011**, *129*, 398–411. [CrossRef]
4. Della Seta, M.; Martino, S.; Scarascia Mugnozza, G. Quaternary sea-level change and slope instability in coastal areas: Insights from the Vasto Landslide (Adriatic coast, central Italy). *Geomorphology* **2013**, *201*, 462–478. [CrossRef]
5. Ietto, F.; Perri, F.; Fortunato, G. Lateral spreading phenomena and weathering processes from Tropea area (Calabria, southern Italy). *Environ. Earth Sci.* **2015**, *73*, 4595–4608. [CrossRef]
6. Agnesi, V.; Rotigliano, E.; Tammaro, U.; Cappadonia, C.; Conoscenti, C.; Obrizzo, F.; Di Maggio, C.; Luzio, D.; Pingue, F. GPS monitoring of the Scopello (Sicily, Italy) DGSD phenomenon: Relationships between surficial and deep-seated morphodynamics. In *Engineering Geology for Society and Territory*; Lollino, G., Giordan, D., Crosta, G.B., Corominas, J., Azzam, R., Wasowski, J., Sciarra, N., Eds.; Springer: Cham, Switzerland, 2015; Volume 2, pp. 1321–1325.
7. Furlani, S.; Devoto, S.; Biolchi, S.; Cucchi, F. Factors triggering sea cliff instability along the slovenian coasts. *J. Coast. Res.* **2011**, *61*, 387–393. [CrossRef]
8. Del Soldato, M.; Confuorto, P.; Bianchini, S.; Sbarra, P.; Casagli, N. Review of works combining GNSS and InSAR in Europe. *Remote Sens.* **2021**, *13*, 1684. [CrossRef]
9. Devoto, S.; Biolchi, S.; Bruschi, V.M.; Furlani, S.; Mantovani, M.; Piacentini, D.; Pasuto, A.; Soldati, M. Geomorphological map of the NW Coast of the Island of Malta (Mediterranean Sea). *J. Maps* **2012**, *8*, 33–40. [CrossRef]
10. Devoto, S.; Biolchi, S.; Bruschi, V.M.; Díez, A.G.; Mantovani, M.; Pasuto, A.; Piacentini, D.; Schembri, J.A.; Soldati, M. Landslides along the North-West Coast of the Island of Malta. In *Landslide Science and Practice*; Margottini, C., Canuti, P., Sassa, K., Eds.; Springer: Berlin/Heidelberg, Germany, 2013; Volume 1, pp. 57–63.
11. Main, G.; Schembri, J.; Gauci, R.; Crawford, K.; Chester, D.; Duncan, G. The hazard exposure of the Maltese Islands. *Nat. Hazards* **2018**, *92*, 829–855. [CrossRef]
12. Soldati, M.; Devoto, S.; Prampolini, M.; Pasuto, A. The spectacular landslide-controlled Landscape of the Northwestern Coast of Malta. In *Landscapes and Landforms of the Maltese Islands*; Gauci, R., Schembri, J.A., Eds.; Springer: Cham, Switzerland, 2019; pp. 167–178.
13. Prampolini, M.; Gauci, R.; Micallef, A.S.; Selmi, L.; Vandelli, V.; Soldati, M. Geomorphology of the north-eastern coast of Gozo (Malta, Mediterranean Sea). *J. Maps* **2018**, *14*, 402–410. [CrossRef]

14. Furlani, S.; Gauci, R.; Devoto, S.; Schembri, J.A. Filfla: A case study of the effect of target practice on coastal landforms. In *Landscapes and Landforms of the Maltese Islands*; Gauci, R., Schembri, J.A., Eds.; Springer: Cham, Switzerland, 2019; pp. 261–271.
15. Pasuto, A.; Soldati, M. Rock spreading. In *Landslide Recognition: Identification, Movement and Courses*; Dikau, R., Brunsden, D., Schrott, L., Ibsen, M.-L., Eds.; Wiley: Chichester, UK, 1996; pp. 122–136.
16. Ibsen, M.-L.; Brunsden, D.; Bromhead, E.; Collison, A. Block slide. In *Landslide Recognition: Identification, Movement and Courses*; Dikau, R., Brunsden, D., Schrott, L., Ibsen, M.-L., Eds.; Wiley: Chichester, UK, 1996; pp. 64–77.
17. Agliardi, F.; Crosta, G.; Zanchi, A. Structural constraints on deep-seated slope deformation kinematics. *Eng. Geol.* **2001**, *59*, 83–102. [CrossRef]
18. Pánek, T.; Klimeš, J. Temporal behavior of deep-seated gravitational slope deformations: A review. *Earth-Sci. Rev.* **2016**, *156*, 14–38. [CrossRef]
19. Mariani, G.S.; Zerboni, A. Surface geomorphological features of deep-seated gravitational slope deformations: A look to the role of lithostructure (N Apennines, Italy). *Geosci. J.* **2020**, *10*, 334. [CrossRef]
20. Devoto, S. Cartografia, Monitoraggio e Modellizzazione di Frane Lungo la Costa Nord-Occidentale dell'isola di Malta. Ph.D. Thesis, University of Modena and Reggio Emilia, Modena, Italy, 3 April 2013.
21. Mantovani, M.; Devoto, S.; Forte, E.; Mocnik, A.; Pasuto, A.; Piacentini, D.; Soldati, M. A multidisciplinary approach for rock spreading and block sliding investigation in the north-western coast of Malta. *Landslides* **2013**, *10*, 611–622. [CrossRef]
22. Devoto, S.; Macovaz, V.; Mantovani, M.; Soldati, M.; Furlani, S. Advantages of using UAV digital photogrammetry in the study of slow-moving coastal landslides. *Remote Sens.* **2020**, *12*, 3566. [CrossRef]
23. Scerri, S. Sedimentary evolution and resultant geological landscapes. In *Landscapes and Landforms of the Maltese Islands*; Gauci, R., Schembri, J.A., Eds.; Springer: Cham, Switzerland, 2019; pp. 31–47.
24. Baldassini, N.; Di Stefano, A. Stratigraphic features of the Maltese Archipelago: A synthesis. *Nat. Hazards* **2017**, *86*, 203–231. [CrossRef]
25. Soldati, M.; Barrows, T.T.; Prampolini, M.; Fifield, K.L. Cosmogenic exposure dating constraints for coastal landslide evolution on the Island of Malta (Mediterranean Sea). *J. Coast. Conserv.* **2018**, *22*, 831–844. [CrossRef]
26. Furlani, S.; Antonioli, F.; Biolchi, S.; Gambin, T.; Gauci, R.; Lo Presti, V.; Anzidei, M.; Devoto, S.; Palombo, M.; Sulli, A. Holocene sea level change in Malta. *Quat. Int.* **2013**, *288*, 146–157. [CrossRef]
27. Coratza, P.; Bruschi, V.M.; Piacentini, D.; Saliba, D.; Soldati, M. Recognition and assessment of geomorphosites in Malta at the Il-Majjistral nature and history park. *Geoheritage* **2011**, *3*, 175–185. [CrossRef]
28. Cappadonia, C.; Coratza, P.; Agnesi, V.; Soldati, M. Malta and Sicily joined by geoheritage enhancement and geotourism within the framework of land management and development. *Geosci. J.* **2018**, *8*, 253. [CrossRef]
29. Piacentini, D.; Devoto, S.; Mantovani, M.; Pasuto, A.; Prampolini, M.; Soldati, M. Landslide susceptibility modeling assisted by Persistent Scatterers Interferometry (PSI): An example from the northwestern coast of Malta. *Nat. Hazards* **2015**, *78*, 681–697. [CrossRef]
30. Mantovani, M.; Devoto, S.; Piacentini, D.; Prampolini, M.; Soldati, M.; Pasuto, A. Advanced SAR interferometric analysis to support geomorphological interpretation of slow-moving coastal landslides (Malta, Mediterranean Sea). *Remote Sens.* **2016**, *8*, 443. [CrossRef]
31. Prampolini, M.; Foglini, F.; Biolchi, S.; Devoto, S.; Angelini, S.; Soldati, M. Geomorphological mapping of terrestrial and marine areas, northern Malta and Comino (central Mediterranean Sea). *J. Maps* **2017**, *13*, 457–469. [CrossRef]
32. Panzera, F.; D'Amico, S.; Lotteri, A.; Galea, P.; Lombardo, G. Seismic site response of unstable steep slope using noise measurements: The case study of Xemxija Bay area, Malta. *Nat. Hazards Earth Syst. Sci.* **2012**, *12*, 3421–3431. [CrossRef]
33. Phinn, S.R.; Menges, C.; Hill, G.J.E.; Stanford, M. Optimizing remotely sensed solutions for monitoring, modeling, and managing coastal environments. *Remote Sens. Environ.* **2000**, *73*, 117–132. [CrossRef]
34. Teeuw, R.M. Applications of remote sensing for geohazard mapping in coastal and riverine environments. In *Mapping Hazardous Terrain Using Remote Sensing*; Teeuw, R.M., Ed.; Geological Society: London, UK, 2007; Special Publications; Volume 283, pp. 93–106.
35. Troiani, F.; Martino, S.; Marmoni, G.M.; Menichetti, M.; Torre, D.; Iacobucci, G.; Piacentini, D. Integrated field surveying and land surface quantitative analysis to assess landslide proneness in the conero promontory rocky coast (Italy). *Appl. Sci.* **2020**, *10*, 4793. [CrossRef]
36. Galea, P. Central Mediterranean tectonics—A key player in the geomorphology of the Maltese Islands. In *Landscapes and Landforms of the Maltese Islands*; Gauci, R., Schembri, J.A., Eds.; Springer: Cham, Switzerland, 2019; pp. 19–30.
37. Gauci, R.; Inkpen, R. The physical characteristics of limestone shore platforms on the Maltese Islands and their neglected contribution to coastal land use development. In *Landscapes and Landforms of the Maltese Islands*; Gauci, R., Schembri, J.A., Eds.; Springer: Cham, Switzerland, 2019; pp. 343–356.
38. Sammut, S.; Gauci, R.; Inkpen, R.; Lewis, J.J.; Gibson, A. Selmun: A coastal limestone landscape enriched by scenic landforms, conservation status and religious significance. In *Landscapes and Landforms of the Maltese Islands*; Gauci, R., Schembri, J.A., Eds.; Springer: Cham, Switzerland, 2019; pp. 325–341.
39. Selmi, L.; Coratza, P.; Gauci, R.; Soldati, M. Geoheritage as a tool for environmental management: A case study in Northern Malta (Central Mediterranean Sea). *Resources* **2019**, *8*, 168. [CrossRef]

40. Gutiérrez, F.; Guerrero, J.; Lucha, P. A genetic classification of sinkholes illustrated from evaporite paleokarst exposures in Spain. *Environ. Geol.* **2008**, *53*, 993–1006. [CrossRef]
41. ISRM. International society for rock mechanics commission on standardization of laboratory and filed tests: Suggested methods for the quantitative description of discontinuities in rock masses. *Int. J. Rock Min. Sci. Geomech. Abstr.* **1978**, *15*, 319–378. [CrossRef]
42. Bruno, D.E.; Ruban, D.A. Something more than boulders: A geological comment on the nomenclature of megaclasts on extraterrestrial bodies. *Planet. Space Sci.* **2017**, *135*, 37–42. [CrossRef]
43. Ruban, D.A. Finding coastal megaclast deposits: A virtual perspective. *J. Mar. Sci. Eng.* **2020**, *8*, 164. [CrossRef]
44. Cruden, D.M.; Varnes, D.J. Landslide types and processes. *Spec. Rep. Natl. Acad. Sci. Transp. Res. Board* **1996**, *247*, 36–75.
45. Walstra, J.; Chandler, J.; Dixon, N.; Dijkstra, T.A. Aerial photography and digital photogrammetry for landsliding monitoring. In *Mapping Hazardous Terrain Using Remote Sensing*; Teeuw, R.M., Ed.; Geological Society: London, UK, 2007; Special Publications; Volume 283, pp. 53–63.
46. Young, A.P.; Carilli, J.E. Global distribution of coastal cliffs. *Earth Surf. Process. Landf.* **2019**, *44*, 1309–1316. [CrossRef]